Batteries & Supercaps

Chemistry Europe
European Chemical Societies Publishing

Accepted Article

Title: Enhancing the Capacitance of Poly(Heptazine Imide) Electrodes in Aqueous Electrolytes via Hybrid Material Design

Authors: Marius Hermesdorf, Ulrich Haagen, Ping Feng, Christof Neumann, Andrey Turchanin, Yan Lu, and Desirée Leistenschneider

To be cited as: *Batteries & Supercaps* **2025**, e202500285

Link to VoR: https://doi.org/10.1002/batt.202500285

WILEY VCH

10.1002/batt.202500285

WILEY VCH

RESEARCH ARTICLE

Enhancing the Capacitance of Poly(Heptazine Imide) Electrodes in Aqueous Electrolytes via Hybrid Material Design

Marius Hermesdorf[1], Ulrich Haagen[1], Ping Feng[1,2], Christof Neumann[3], Andrey Turchanin[3,4], Yan Lu[1,2,5], and Desirée Leistenschneider[1,4]*

1 M. Hermesdorf, U. Haagen, P. Feng, Prof. Dr. Y. Lu, Dr. D. Leistenschneider
Institute for Technical Chemistry and Environmental Chemistry
Friedrich-Schiller University Jena
Philosophenweg 7a, 07743 Jena (Germany)
E-mail: desiree.leistenschneider@uni-jena.de

2 P. Feng, Prof. Dr. Y. Lu
Institute of Electrochemical Energy Storage
Helmholtz-Zentrum Berlin für Materialien und Energie
Hahn-Meitner-Platz 1, 14109, Berlin, Germany

3 Dr. C. Neumann, Prof. Dr. A. Turchanin
Institute of Physical Chemistry
Friedrich-Schiller University Jena
Lessingstraße 10, 07743 Jena, Germany

4 Dr. D. Leistenschneider, Prof. Dr. A. Turchanin
Center for Energy and Environmental Chemistry Jena (CEEC Jena)
Friedrich-Schiller University Jena
Philosophenweg 7a, 07743 Jena, Germany

5 Prof. Dr. Y. Lu
Helmholtz Institute for Polymers in Energy Applications Jena (HIPOLE Jena)
07743 Jena, Germany.

Supporting information for this article is given via a link at the end of the document.

Abstract: Potassium poly(heptazine imide) (K-PHI), an ionic carbon nitride, has gathered interest as functional material in energy conversion, in particular as photocatalyst. As a semiconductor, it lacks of electric conductivity. Paired with its low surface area, its potential is limited for electric and adsorption-based applications. This work reports the design of a PHI/carbon hybrid using micro- and mesoporous carbon as support in order to increase electric conductivity and the electrochemically-active surface area of K-PHI. By that, the specific surface area (SSA) is increased from 9 $m^2 g^{-1}$ in bulk K-PHI up to 312 $m^2 g^{-1}$ when designing the mesoporous hybrid. Furthermore, TEM images indicate a growth of K-PHI within the mesopores of the carbon, whereas the microporous hybrid exhibits K-PHI at the external surface. Both hybrids show enhanced capacitance up to 23 F g^{-1} compared to 2 F g^{-1} for bulk K-PHI. The mesoporous hybrid also shows enhanced capacitance retention at higher specific currents as the open mesopores enable faster ion diffusion combined with increased electric conductivity and shorter dielectric relaxation times. Overall, the design of K-PHI@carbon hybrids enables the study of electrochemical processes at the PHI surface without being limited by its low electric conductivity and low surface area.

Introduction

With the development of the transistor in 1947, society entered the Information Age and ever since the demand for electrical energy storage devices is steadily increasing.[1] Additionally, the shift towards renewable energy production and an increasingly environmentally conscious society leads to the advancement of electrified technical processes like catalysis. With that, also the advancement of abundant electrode materials, in particular, with adjustable physical and chemical properties is needed. Potassium poly(heptazine imide) (K-PHI) is an ionic, polymeric carbon nitride, consisting of C, N, K and H, which are among the most abundant elements on earth. Due to its semiconducting behavior it draws a lot of attention as noble metal-free photocatalyst.[2, 3] Typically, K-PHI is prepared by polymerizing nitrogen-rich precursors in an ionothermal synthesis using K-containing salts. The structure of K-PHI consists of layers of heptazine units, which are connected via deprotonated imide bridges. The negative charge is compensated by K^+ counterions derived from the salt melt.[2, 4-6] PHIs are also referred to as "organic zeolites", as K^+ can be easily exchanged with protons or other metal cations such as Li^+, Na^+, or even redox-active transition metal cations such as Fe^{2+} or Co^{2+}.[7, 8]

As a semiconducting material, PHI has only scarcely been investigated as electron-conductive or redox-active material in electrochemical energy storage devices. The work of Lotsch *et al*. i.e. recently highlights the material in the context of novel solar battery systems, in which K-PHI enables a charge separation under light illumination. This further enhances the energy density of the solar battery device.[9] In the context of supercapacitors, the material has not yet been discussed, although its cation conductivity, in particular in aqueous media, makes it an interesting candidate for high power energy storage devices.[10] Additionally, there is a great potential to develop new electrode materials by modifying the negatively charged imide bridges with electrochemically-active cationic species. Previous studies on the

10.1002/batt.202500285

RESEARCH ARTICLE

interaction of PHI with ionic liquid cations showed that the presence of $EMIM^+$ can enable charge accumulation and stabilizes charge separation for a longer period of time under light irradiation.[11] So far, there is no understanding of how cations from electrolytes interact with the negatively charged imide bridges under the presence of an electrochemical potential. The formation of an electric double-layer and the capacitive properties of PHI materials in different aqueous electrolytes are still rarely known. This is surprising because the structure of these materials is suitable to establish ion storage concepts which are not covered by ordinary porous electrode materials solely based on traditional electrostatic sorption such as porous carbons.

The two main reasons are low electric conductivity and their low detectable specific surface area. The high internal electrode resistance does not allow to study voltage-induced charge transfer mechanisms or to investigate how imide-cations within the network exchange with cations from the electrolyte without being affected by the high resistance of the system. This is a well-known challenge also for other carbon nitride-based supercapacitor electrodes.[12, 13] In terms of porosity of K-PHI the highest reported specific surface area of PHIs is about 105 m^2g^{-1}.[14] Generally, increasing this surface area could lead to an increased energy density and facilitate the analysis of the electrochemical processes at its interface. Additionally, in PHIs as N-rich compounds that consist of Lewis acidic and basic sites, capacitance may not correlate linearly with the surface area as it is usually assumed. Generally, the surface area is determined from the Brunauer-Emmett and Teller theory based on the assumption of the monolayer formation of physically adsorbed N_2 molecules. Comparably, the electric double-layer is assumed to consist of electrostatically adsorbed electrolyte ions at the electrode surface. If there are stronger ion-electrode interactions, i.e. the formation of Lewis adducts, it may be possible that the capacitance is increased, although the surface area may not be larger due to the smaller distance of ions and electrode surface. Because the electric double-layer capacitance of PHIs could not yet be investigated due to the aforementioned reasons, this is a completely new research field and its potential for further development is yet to be estimated.

An effective way to address this is by designing hybrid materials. As a rather new material PHI has not been reported as a hybrid active material for electrochemical storage devices, yet. However, since carbon nitrides are known for nearly 200 years[15] a great variety of research on carbon nitride containing hybrids for supercapacitors has already been published. There are numerous insightful review articles dealing with synthesis strategies and application of carbon nitride hybrids as active materials in different energy storage devices.[16-19] Among others, carbon allotropes are well established as component in hybrid design and as electrodes in supercapacitors due to their high electric conductivity, high chemical stability combined with adjustable pore structures, and hence high specific surface areas.[20, 21] Therefore, graphene, carbon nanotubes and other porous carbons are explored as support for carbon nitride hybrid materials.[12, 22-24] The synthesis approaches are also applied for similar nitrogen-rich carbons, as *Oschatz et al*. reported a nanocomposite of condensed hexaazatriphenylene-hexacarbonitrile (HAT-CN) incorporated in a mesoporous carbon material.[25] Thereby, the ion storage capacity and rate capability of the sodium ion capacitors by decoupling the ion storage and the electron transport could be significantly enhanced.

Within this work, porous carbon was chosen as support material to design hybrids with K-PHI. The generation of such hybrid material will pave the way for the application of this material class in EDLCs and other electrochemical technologies. The aim of this work is to establish a synthesis procedure for M-PHI@carbon hybrid materials with lower electric resistance and increased electrochemically active surface area. As a consequence, the final capacitance of PHI materials will be increased. Moreover, it will be possible to further investigate the electrochemical interaction of PHIs with electrolyte cations, and to further understand their electrochemical behavior in electrolytes containing different cation species without the overlapping influence of high electric resistance.

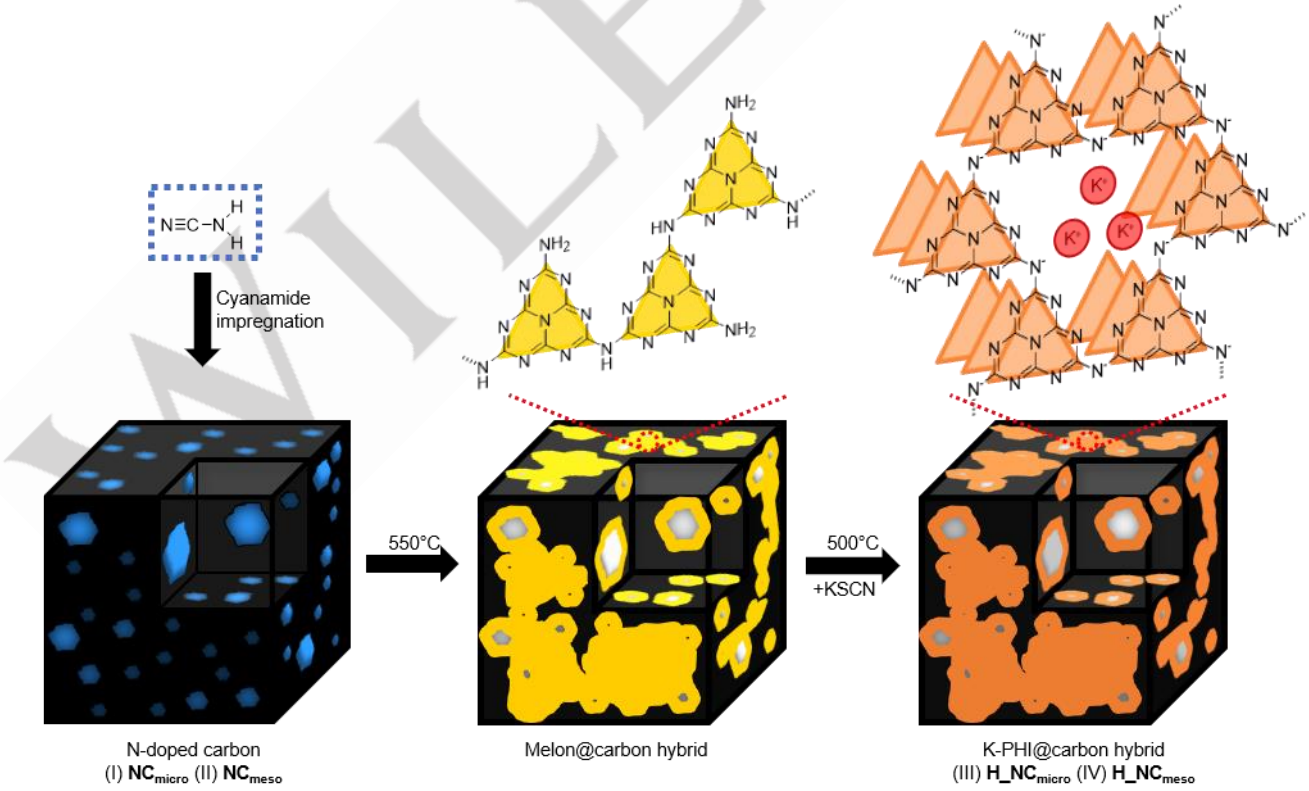

Scheme 1: General synthesis route for impregnation of nitrogen-doped carbons NC_{micro} and NC_{meso} with cyanamide and subsequent hybrid synthesis to H_NC_{micro} and H_NC_{meso}.

10.1002/batt.202500285
WILEY VCH

RESEARCH ARTICLE

Results and Discussion

Influence of porosity

As carbon support material, two N-doped porous carbons referred to as NC_{micro} and NC_{meso}, were prepared. For the carbon synthesis a methyl-cellulose as carbon source was treated in a ball mill with melamine as nitrogen dopant for heteroatom functionalization and K_2CO_3 as activation agent.[26] To introduce larger mesopores in NC_{meso} ZnO nanoparticles were added as a hard template.[25] Since NC_{micro} and NC_{meso} only differ in pore structure, they are an ideal model system to investigate the effect of pore size on the K-PHI@carbon hybrid. The nitrogen functionalization is speculated to have a beneficial impact on the hybrid synthesis. Since K-PHI is a polar material with high nitrogen content, the functionalized surface of both carbon supports could improve the strength of the junction between K-PHI and the carbon support. The approach for the hybrid synthesis is depicted in Scheme 1. First, the carbon support is impregnated with cyanamide as K-PHI precursor.[6] Cyanamide is subsequently converted to the bulk carbon nitride melon before forming K-PHI within the carbon framework by ionothermal synthesis in a KSCN melt.[5]

Following the synthesis of the two nitrogen-doped carbons NC_{micro} and NC_{meso}, the respective hybrids H_NC_{micro} and H_NC_{meso} and bulk K-PHI as reference the pore structure and porosity changes were analyzed by Ar-physisorption. The isotherm of NC_{micro} in Figure 1a displays the typical shape of type Ib characteristic for a predominantly microporous material.[27] NC_{micro} exhibits a pore size distribution with pore diameters ranging from 1-3 nm containing also narrow mesopores. The isotherm of NC_{meso} can be classified as type IVa identifying it as a mesoporous material.[27] While also containing micropores of just below 2 nm, the majority of the porosity is derived from mesopores with diameters up to 7 nm. With 1.97 $cm^3\,g^{-1}$, NC_{meso} has the higher pore volume due to larger mesopores compared to the pore volume of 1.27 $cm^3\,g^{-1}$ of NC_{micro}, which is due to the use of the hard template. Regarding the specific surface area, the trend is reversed because the higher amount of micropores in NC_{micro} lead to a higher surface area of 2485 $m^2\,g^{-1}$ in contrast to 2257 $m^2\,g^{-1}$ for NC_{meso}. The values for the porosity and the specific surface area for each material are summarized in Table S1 in the supporting information. Thus, the synthesis of micro- and mesoporous carbons was successful and will be used to discuss the influence of porosity on the hybrid formation with K-PHI.

In a next step, all carbon materials were further treated with cyanamide and KSCN to grow PHI on their surface. First, the carbons were infiltrated with cyanamide as a carbon nitride forming precursor. This first infiltration step yields a hybrid of carbon and the linear C_3N_4 polymer, the so-called melon.[6] According to N_2-physisorption results shown in Figure S1, the surface area of NC_{meso} is reduced from 2257 $m^2\,g^{-1}$ to 99 $m^2\,g^{-1}$ after the conversion to melon. The formation of the carbon nitride is also evidenced by elemental analysis because the nitrogen content increases up to 42.1 wt.% as shown in Table S2. This points to an infiltration of the K-PHI precursor inside the pores of the carbon. This reduction of the specific surface area can also be observed for NC_{micro}. In this case, since the carbon material exhibits smaller pores, the whole porosity is filled or blocked by melon. After ionothermal synthesis, both hybrid materials show a decreased porosity leading to decreased surface area compared to the porous carbon (Figure 1b).

The specific surface area of NC_{meso} is reduced from 2257 $m^2\,g^{-1}$ to 312 $m^2\,g^{-1}$ after the conversion to H_NC_{meso}. The same trend but even more pronounced can be observed for the NC_{micro} and H_NC_{micro}. The hybrid material based on the microporous carbon only has a surface area of 26 $m^2\,g^{-1}$. It seems that, comparable to the first impregnation step, the smaller micropores are either completely filled or blocked by the formation of K-PHI. However, compared to bulk K-PHI H_NC_{meso} displays a significant larger surface area and porosity. Hence, the Ar-physisorption isotherms give a first indication that larger mesopores in the support material are beneficial for the incorporation of K-PHI, while also maintaining a higher surface area, which will be beneficial for the later electrochemical application. Besides the decrease in surface area the K-PHI formation in the hybrid materials is expected to largely affect the bulk and surface composition as well as surface functionality. Hence, all synthesized materials were analyzed using both XPS and elemental analysis. The compositional data derived from XPS survey spectra and elemental analysis are summarized in Table 1. The fitted high resolution (HR) spectra of both carbon support materials are displayed in Figure S2. NC_{micro} and NC_{meso} have a N content of 3.2 wt.% and 5.7 wt.%, respectively, according to elemental analysis, matching with the 4.0 wt.% and 4.4 wt.% derived from XPS compositional analysis. According to the N1s XPS spectra in Figure S2, NC_{micro} as well as NC_{meso} exhibit mainly pyrrolic (400.2 eV) and pyridinic (398.6 eV) functional groups. At higher binding energies both show a third peak associated with higher oxidized N functional groups.[26]

XPS results also indicate the comparable functionalization of NC_{micro} and NC_{meso}. It is speculated that the pyridinic and pyrrolic N-functionalities in NC_{micro} and NC_{meso} will facilitate the anchoring of K-PHI on the electrically conductive carbon. K-PHI consists of heptazine units and their inhomogeneous electron density distribution matches well with the polarity of the N-functionalized carbons. The C1s spectra for both carbons in Figure S2 a) and d), respectively, show nearly identical peaks. Both NC_{micro} and NC_{meso} show dominant peaks at 284.5 eV and 284.6 eV in relation to C-C bonding motifs from the porous carbon.

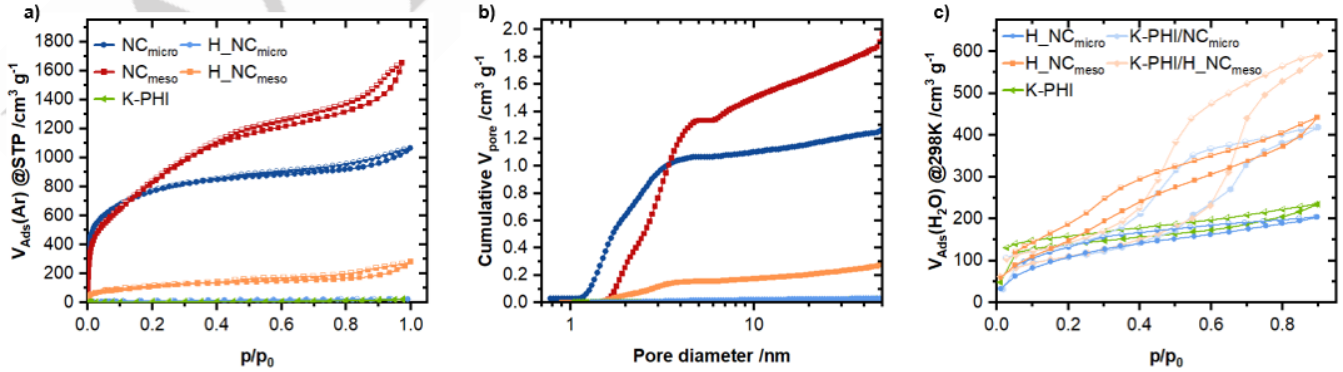

Figure 1: a) Ar-physisorption isotherms measured at 87 K of NC_{micro}, NC_{meso}, H_NC_{micro} and H_NC_{meso}. b) Cumulative pore volume derived from Ar-physisorption at 87 K. c) H_2O vapor physisorption isotherms of bulk K-PHI, H_NC_{micro}, H_NC_{meso} and the corresponding physical mixtures K-PHI/NC_{micro} and K-PHI/NC_{meso} (K-PHI to Carbon 70:30 wt%).

10.1002/batt.202500285

RESEARCH ARTICLE

Table 1: Compositional data in wt.% for nitrogen-doped porous carbons NC_{micro} and NC_{meso} and hybrid materials H_NC_{micro} and H_NC_{meso}.

	C [1] wt.%	N wt.%]	O [1] wt.%	K [1] wt.%	C [2] wt.%	H [2] wt.%]	N [2] wt.%	S [2] wt.%	C/N [2]
NC_{micro}	88.8	4.0	7.2	0	89.2	0.4	3.2	0	27.9
NC_{meso}	84.8	4.4	10.8	0	82.7	0.5	5.7	0	14.5
H_NC_{micro}	25.4	43.3	7.4	22.3	43.7	1.0	32.1	1.1	1.4
H_NC_{meso}	47.7	35.5	3.8	11.9	44.2	1.1	33.1	0	1.3

1 derived from XPS survey spectra. 2 derived from elemental analysis.

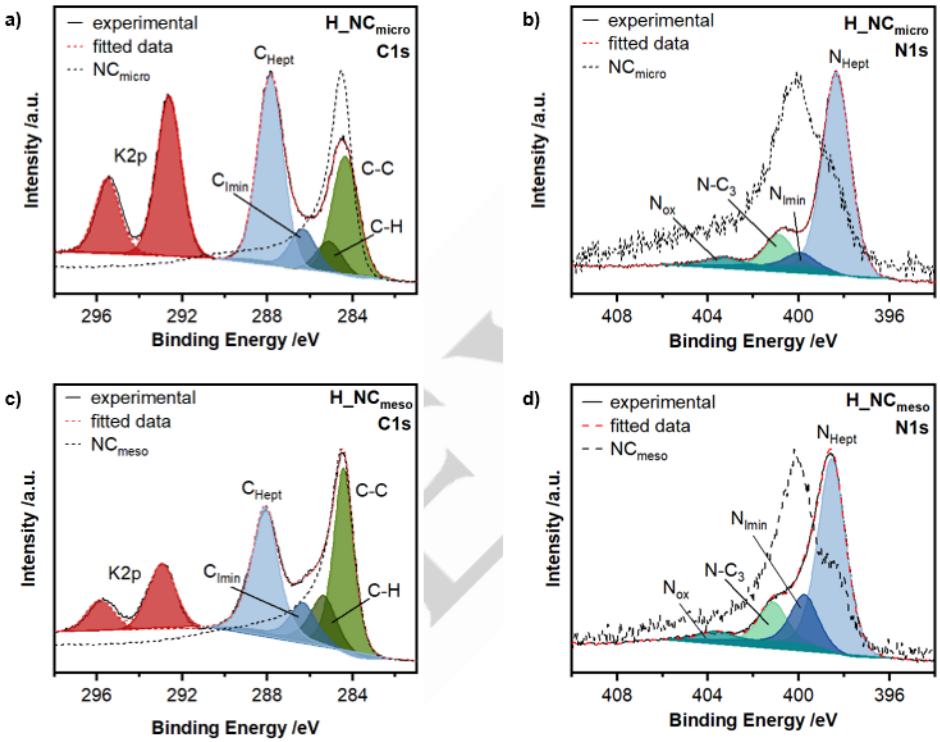

Figure 2: Fitted C1s and N1s HR-XPS spectra of H_NC_{micro} and H_NC_{meso} with respective carbon as reference.

The peaks at higher binding energies are derived from different oxygen and nitrogen containing functional groups, as confirmed also by O1s spectra. The HR C1s and N1s spectra of both hybrids are displayed in Figure 2.

Compared to the respective carbon support (displayed here as dotted line in each spectrum), H_NC_{micro} and H_NC_{meso} display significant differences. In the C1s spectra the most notable change is the appearance of a dominant peak at 287.9 eV and 288.1 eV, respectively. This peak is caused by carbon in the heptazine units of K-PHI. Additionally, a second peak at 286.3 eV evolved, which can be assigned to C-NH_2 or C-OH groups.[28] The peaks in the lower binding energy region can be connected with C-C at 284.4 eV and C-H bonding motifs at 285.1 eV, respectively, and 285.4 eV from the carbon support. One distinct difference between both hybrid materials in the C1s spectrum is the position of the peak with highest intensity. In H_NC_{meso} the peak with the highest intensity is related to the carbon support NC_{meso} at 284.4 eV. In contrast, the most intense peak for H_NC_{micro} is associated with carbon from the heptazine framework at 287.9 eV which indicates a higher amount of K-PHI on the surface of H_NC_{micro}. The doublets in the binding energy region of both C1s HR spectra result from the K2p core electrons of potassium ions present in K-PHI. These observations are supported by the compositional data derived from the survey spectrum**.** XPS compositional analysis shows distinct differences between H_NC_{meso} and the other two materials. For instance, H_NC_{micro} has close to double the amount of nitrogen content (43.4 wt.%) compared to carbon (25.4 wt.%). However, for H_NC_{meso} this trend is reversed since it has a higher detected carbon content. This further indicates that K-PHI is more concentrated on the external surface in H_NC_{micro} than in H_NC_{meso}, where it is located preferably within the internal pores and is then not entirely detected via XPS as a surface sensitive method. The potassium content supports the trend, too, being twice as high for H_NC_{micro}. Furthermore, the XPS results are in line with Ar-physisorption since the low gas uptake of H_NC_{micro} suggested that the pores of the carbon support are not accessible for the gas anymore after K-PHI formation while a significant volume of open pores remained in H_NC_{meso}. After the hybrid synthesis the counts of the N1s signal are significantly higher due to an increase in nitrogen content. The most intense peak at 398.3 eV and 398.5 eV, respectively, is derived from the nitrogen from C-N=C groups in

10.1002/batt.202500285

RESEARCH ARTICLE

the heptazine unit. Further peaks can be assigned to imine bridges at around 400 eV and to quaternary N-C_3 groups at ca. 401 eV.[29] Overall, the N1s spectra demonstrate a comparable nitrogen functionalization on the surface of both hybrid materials. Additionally, while XPS might suggest a higher amount of K-PHI on the surface of H_NC_{micro}, elemental analysis as a bulk method confirms a comparable heteroatom content in both hybrids with almost the same C/N ratio. This further strengthens the assumption, that K-PHI is more likely formed within the pores of the mesoporous carbon, whereas it forms at the outer surface when using a microporous carbon.

To further investigate the modification of the surface after the hybrid synthesis, H_2O-vapor physisorption isotherms were measured. It is speculated, that in case of confined K-PHI, which is known to strongly interact with water as bulk material, the water adsorption behavior of the respective hybrid is altered. Therefore, water vapor adsorption will help to distinguish whether the synthesized materials act as a true hybrid material or as a physical mixture of the respective bulk materials. Moreover, the accessibility of the pores for aqueous species can be judged, as well, which is crucial to discuss the accessibility of the PHI surface for electrolyte species. The H_2O-vapor isotherms of bulk K-PHI, both hybrids and the respective physical mixtures are presented in Figure 1c. The physical mixtures were prepared by estimating the ratio of K-PHI and carbon support in the hybrids based on the elemental analysis results listed in Table 1. By using both carbon and nitrogen content of K-PHI and the respective carbon the relative contribution of each component in H_NC_{micro} and H_NC_{meso} was calculated. Both hybrids were estimated to consist of around 70 wt.% K-PHI and 30 wt.% of the respective carbon. As a reference, PXRD and elemental analysis of the physical mixtures was measured with nearly identical C/N ratios which can be found in the supporting information in Figure S3 and S4, respectively (denoted as K-PHI/H_NC_{micro} and K-PHI/H_NC_{meso}). First, the isotherms of both carbon support materials are shown in Figure S1b and confirm the comparable polarity of NC_{micro} and NC_{meso} as the water uptake is close to identical until relative pressures above 0.6. Only the overall water uptake differs due to the different carbon pore volumes. K-PHI is known to be highly hydrophilic, while carbons, even though doped with nitrogen, are known to be rather hydrophobic.[30] This is also the case for NC_{micro} and NC_{meso}, as they give S-shaped isotherms. Generally, the onset of water uptake of both carbons is located at relatively low relative pressure compared to non-doped carbons.[31] When comparing the hybrids H_NC_{micro} and H_NC_{meso} to the respective carbon and the bulk K-PHI, it is apparent that the isotherm resembles the form of hydrophilic K-PHI. Both isotherms show an immediate uptake in the low relative pressure region. Compared to the physical mixture of K-PHI and NC_{micro}, the hybrid H_NC_{micro} exhibits a low porosity and a water uptake comparable to bulk K-PHI. This further strengthens a completely blocked carbon microporosity, which cannot adsorb any water. Only K-PHI on the outer surface adsorbs water, which explains the similarity to the water isotherm of bulk K-PHI. In contrast, H_NC_{meso} has a steady water vapor uptake also at higher relative pressures where water-water interactions in the remaining open porosity become dominant. Compared to the pure carbon material, the water uptake is lower, which can also be explained by the generally lower porosity and pore volume. Compared to its physical mixture reference, the isotherm indicates a true hybrid material. The hybrid material does not exhibit an S-shaped isotherm with an immediate water uptake at low p/p_0. Compared to bulk K-PHIs, H_NC_{meso} behaves as a hydrophilic material with larger porosity, which can be beneficial for K-PHI applications that require higher specific surface areas. Moreover, it proves that the surface of K-PHI is accessible for aqueous species. Since K-PHI is a crystalline material, the hybrids were further structurally characterized using PXRD. While the diffractograms of the amorphous carbons show no distinct reflexes, H_NC_{micro} and H_NC_{meso} show an PXRD pattern comparable to bulk K-PHI as can be seen in Figure 3a.

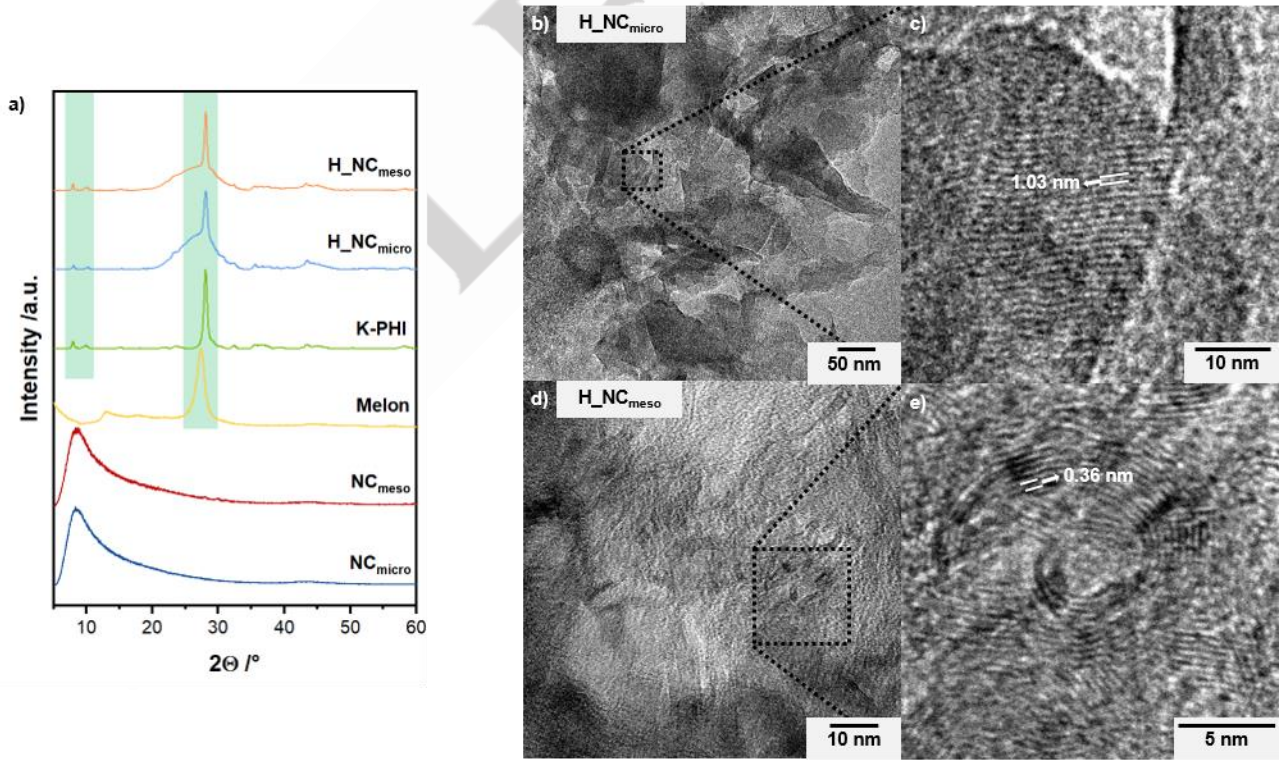

Figure 3: a) PXRD of K-PHI, H_NC_{micro} and H_NC_{meso}. b) TEM image of H_NC_{micro}. c) Zoom into TEM image of H_NC_{micro}. d) TEM image of H_NC_{meso}. e) Zoom into TEM image of H_NC_{meso}.

10.1002/batt.202500285

RESEARCH ARTICLE

The hybrid materials, as well as bulk K-PHI display two reflexes in the low 2Θ-region at 7.9° ($\bar{1}10$) and 9.9° (010). These reflexes can be ascribed to the in-plane reflexes of K-PHI.[5] The in-plane reflexes in the low 2Θ region also help to distinguish between K-PHI and bulk carbon nitride melon. Both hybrids show the most dominant reflex at 27.9° originating from the stacked layers of K-PHI as it is typical for 2D-layered materials.[5] While the pattern of melon also displays a stacking reflex it is notably broader and shifted to a lower 2Θ value of 27.4° indicating the wider interlayer distance in the K-PHI precursor. Both H_NC$_{micro}$ and H_NC$_{meso}$ show a very broad shoulder in the region from ca. 20°-30° 2Θ which can be ascribed to the amorphous carbon support. Though the crystallinity in the hybrids in general appears to be lower compared to bulk PHI, the PXRD patterns confirm the presence of K-PHI within the materials.

The morphology of the prepared materials was analyzed by scanning electron microscopy (SEM). The images of the porous carbon support materials are shown in Figure S4. Both carbon support materials have a rough, unordered surface typical for amorphous materials. The morphology of the hybrids is changed as the surface appears to be smoother. Considering results from XPS and PXRD the SEM images show the formed K-PHI in the hybrid materials. From the images no apparent difference between H-NC$_{micro}$ and H_NC$_{meso}$ is observed. However, based on the Ar-physisorption and XPS analysis, it is speculated that H_NC$_{micro}$ consists of externally coated K-PHI that blocks micropores, whereas H_NC$_{meso}$ could exhibit K-PHI that is located within the mesoporosity. Therefore, transmission electron microscopy (TEM) images of H_NC$_{micro}$ and H_NC$_{meso}$ and the respective carbons were recorded (Figure 3). As expected from PXRD, the TEM images of NC$_{micro}$ and NC$_{meso}$ display only amorphous, disordered character, while bulk K-PHI shows domains with a long-range order as shown in Figure S5. It is noteworthy to mention, that the beam damages K-PHI instantly during the measurement, which complicates the collection of high-resolution images of its crystalline structure.

The typical stacking of K-PHI layers, which was also identified in the PXRD patterns of the hybrids, is also observed in the TEM image of H_NC$_{micro}$ shown in Figure 3b. The TEM images of K-PHI and H_NC$_{micro}$ resemble each other, strengthening the assumption of externally coated K-PHI on the carbon support. Also, homogenous areas, which resemble NC$_{micro}$ are observed (Figure 3b), indicating a phase separation of K-PHI and the carbon. For H_NC$_{micro}$ the lattice fringes correspond to a 1.03 nm distance. The distance matches with the in-plane reflex observed in the diffractogram at 8.0 2 Θ. For H_NC$_{meso}$ it was possible to obtain TEM images in a higher resolution without an immediate damage of the hybrids structure, which points to less charging during the measurement (Figure 3d). It appears that the lattice fringes of K-PHI exhibit a curved orientation instead of the straight stacking of the material in bulk. The distance between the layers based on TEM was calculated to be 0.36 nm which matches the range of previously reported interlayer distance of K-PHI layers. Keeping in mind the results from Ar-physisorption experiment, the cumulative pore volume showed some open mesopore volume for H_NC$_{meso}$. Therefore, the TEM images indicate the growth of K-PHI around the mesopore walls in H_NC$_{meso}$. Finally, it can be assumed that the micropores of carbon are too small to grow PHI within the pores, which further leads to external PHI growth. Mesoporous carbons, on the other hand, can be used to generate PHIs that are growing within pores. This leads to the formation of PHI with a higher surface area due to curved stacked layers compared to a bulk PHI. To the best of our knowledge, a PHI confined into the mesopores of a porous carbon, leading to curvature of the stacked layers has not been reported yet.

Electric double-layer investigation

The hypothesis of this work is, that the introduction of K-PHI into the porous carbon matrix increases the electric conductivity and surface area, thus, paves the way for their electrochemical utilization i.e. as electrode materials in EDLCs. To further analyze the electric double-layer formation in PHIs, the hybrid materials as well as bulk K-PHI were investigated in a symmetrical EDLC configuration in 1M KCl. In order to analyze the conductivity properties of the hybrid materials, impedance spectroscopy was measured and the data is shown in Figure 4.

Comparing the data from potentiostatic electrochemical impedance spectroscopy (PEIS) of both hybrids, it is evident that the resistive contributions of bulk K-PHI are significantly decreased (Figure 4a). Though the electrode resistance from the first x-axis intercept is comparable, the diameter of the semicircle is enlarged hinting at lower internal conductivity and higher charge transfer resistance for bulk K-PHI.[32] Furthermore, the resistance is comparable to the Nyquist plot of the pristine carbon support materials NC$_{micro}$ and NC$_{meso}$ pointing to an improved electric conductivity.

The hybrid materials are comparable regarding their high frequency behavior, while the steeper slope for H_NC$_{meso}$ compared to H_NC$_{micro}$ could indicate faster equilibration of the electric double-layer formation in the system. It is noteworthy, that the relative changes are not significant and for a clear evaluation more cells need to be measured to rule out any other influencing cell parameters. Generally, Nyquist plots indicate that the hybrid formation leads to a less delayed current response of the devices when alternating voltage is applied, which could point to faster charge transfer processes within the electrode. This potentially indicates a reduced grain boundary resistance between PHI and N-doped carbon, especially when considering that H_NC$_{micro}$ seems to have similar structural features to K-PHI in terms of open porosity and surface area. The PEIS data was further used to distinguish between real part $C'(\omega)$ and imaginary part $C''(\omega)$ of the capacitance in relation to the frequency according to a model reported by *Fauvarque et al.* for symmetrical supercapacitors. Both parts can be calculated with equation (1) and (2) respectively.[33]

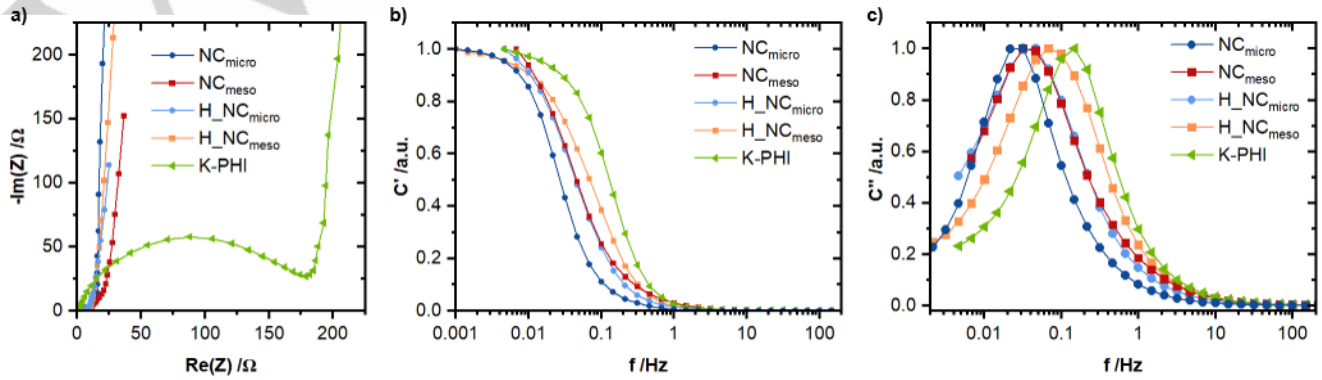

Figure 4: PEIS analysis of symmetrical EDLCs in 1M KCl (1 mHz to 100 kHz) a) Nyquist plot of NC$_{micro}$, NC$_{meso}$, H_NC$_{micro}$, H_NC$_{meso}$ and K-PHI. b) Capacitance evolution depending on frequency. c) Normalized imaginary capacitance in dependence of frequency.

10.1002/batt.202500285

RESEARCH ARTICLE

$$C'(\omega) = \frac{-Z''(\omega)}{\omega|Z(\omega)|^2} \quad (1)$$

$$C''(\omega) = \frac{Z'(\omega)}{\omega|Z(\omega)|^2} \quad (2)$$

The derived normalized plots for the real and imaginary part of the capacitance are shown in Figure 4b and 4c, respectively. Each plot of the imaginary capacitance $C''(\omega)$ goes through a maximum at a frequency f_0 which can be converted to a time constant giving the dielectric relaxation time.[33] As evident, K-PHI has the shortest relaxation time of all materials in 1M KCl while NC_{micro} has the longest. In fact, both hybrids materials show decreased relaxation time compared to the respective porous carbon support. This indicates a positive effect of K-PHI incorporation into the porous carbons when regarding the materials as potential EDLC electrodes. It is generally known that a short dielectric relaxation time is a good indicator for the high-power density of an EDLC electrode material. Thus, filling the porosity of the carbon material with a semiconducting material could potentially enhance the power density of the final EDLC compared to its porous carbon counterpart.

In order to investigate the capacitance of the materials, CV measurements at different scan rates were performed. CVs for the hybrid materials and the respective bulk carbons, as well as bulk K-PHI are compared in Figure 5a and 5b. The specific capacitance of both hybrids is significantly increased compared to K-PHI. It is noteworthy that even H_NC_{micro} demonstrates higher capacitance than bulk K-PHI, although its specific surface area was not increased. Therefore, it is assumed that the hybrid exhibits an improved electric conductivity, which further leads to higher capacitance and electric double-layer formation. Compared to the porous carbons, on the other hand, the capacitance of the hybrids is decreased at low scan rates, which is expected due to their higher surface area.

When looking at the volumetric capacitance, the hybrid materials perform similar to the respective carbon support and for the mesoporous materials the hybrid even slightly outperforms NC_{meso}. As volumetric capacitance is an important supercapacitor manufacturing parameter, those hybrids exemplify how promising PHIs as a material class for EDLCs could be, but are not yet explored as such.

To gain information about the power density of the hybrids, the normalized capacitance retention from CV's was calculated according to equation (3) at various scan rates with m_{AM} being the mass of the active material in one electrode, v as the scan rate and V_1 and V_2 the potential limits of the measurement.

$$C_S = \frac{1}{2 \cdot m_{AM} \cdot \nu (V_2 - V_1)} \int_{V_1}^{V_2} I dV \quad (3)$$

In Figure 5c the normalized capacitance retention is shown while the absolute calculated specific capacitance retention is shown in Figure S6. Looking at the capacitance retention at low scan rates, H_NC_{micro} and H_NC_{meso} show nearly the same specific capacitance of around 22 F g^{-1} with H_NC_{micro} even having a higher value. However, with increasing scan rate, the capacitance of H_NC_{micro} is quickly dropping below the performance of H_NC_{meso}. At 100 mV s^{-1} H_NC_{micro} only remains 20% of the initial capacitance at 2 mV s^{-1}, while H_NC_{meso} still has 45% capacitance retention. This emphasizes the faster equilibration of the electric double-layer at higher scan rates for the mesoporous hybrid material, which was already assumed from the PEIS data. It is assumed that this is due to the presence of mesopores and open porosity, which enable a faster diffusion of ions when polarization is reversed. Moreover, a lower grain boundary resistance could further enhance this capacitance retention. However, H_NC_{meso} even outperforms both porous carbons in terms of capacitance retention at high scan rates. Similar to H_NC_{micro} the capacitance at 100 mV s^{-1} is around 20% of the initial capacitance at lower scan rates for both NC_{micro} and NC_{meso}. Therefore, the surface chemistry of the electrodes containing K-PHI seems to be beneficial for electric double-layer formation, as well. As expected, bulk K-PHI has by far the lowest capacitance. However, similar to H_NC_{meso} it contains most of its initial capacitance at high scan rates and has a relative retention of 40% of its initial capacitance. The steeper decrease in capacitance in H_NC_{micro} especially compared to bulk K-PHI is interesting, as previous structural and chemical characterization suggested similar properties for both materials. Even though Ar-physisorption revealed comparable low surface areas, the CV measurements indicate a significantly higher accessible electrochemical surface area in KCl in H_NC_{micro}. As this area is derived from NC_{micro}, the decay in capacitance can be rationalized with hindered ion movement within the smaller micropores. Combining these results with the dielectric relaxation time from the impedance analysis it is evident that the presence of K-PHI is beneficial for higher power density of the device compared to the pristine porous carbon electrodes. It is further speculated that the presence of potassium ions within K-PHI enables a faster double-layer build-up due to reduced diffusion limitation. Thus, at the same scan rates, the capacitance is higher.

To further strengthen this hypothesis, H_NC_{meso} was tested in different aqueous electrolytes containing different cations, namely 1M LiCl and 1M NaCl (Figure 6).

From the PEIS and CV results shown in Figure 6a and 6b, it is evident that in 1M LiCl the deviation from ideal EDLC behavior is most pronounced. This could originate from lower electrolyte conductivity, as PEIS data points to a comparable electrolyte conductivity for Na and K, and a significantly lower conductivity for LiCl (Figure S7a).[34] Therefore, it is also speculated that the hardness of Li^+ and the strong interaction with water molecules influences the double-layer formation at the surface. While the capacitance at low scan rates for Na and K is comparable at low scan rates the decrease in 1M NaCl is more pronounced compared to KCl.

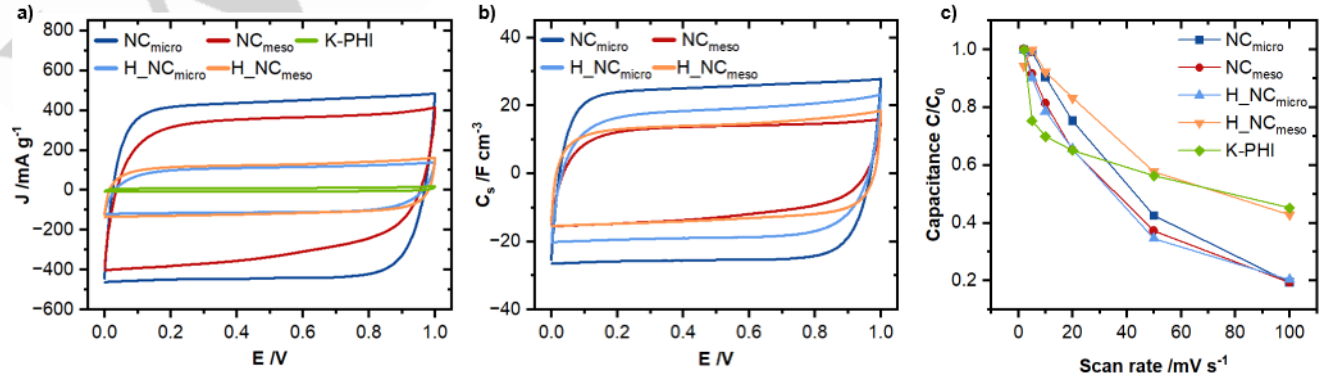

Figure 5: CV analysis of symmetrical EDLC with 1M KCl a) CV of NC_{micro}, NC_{meso}, H_NC_{micro}, H_NC_{meso} and K-PHI at a scan rate v 5 mV s^{-1}. b) Volumetric capacitance against voltage. c) Normalized capacitance retention for different scan rates.

10.1002/batt.202500285

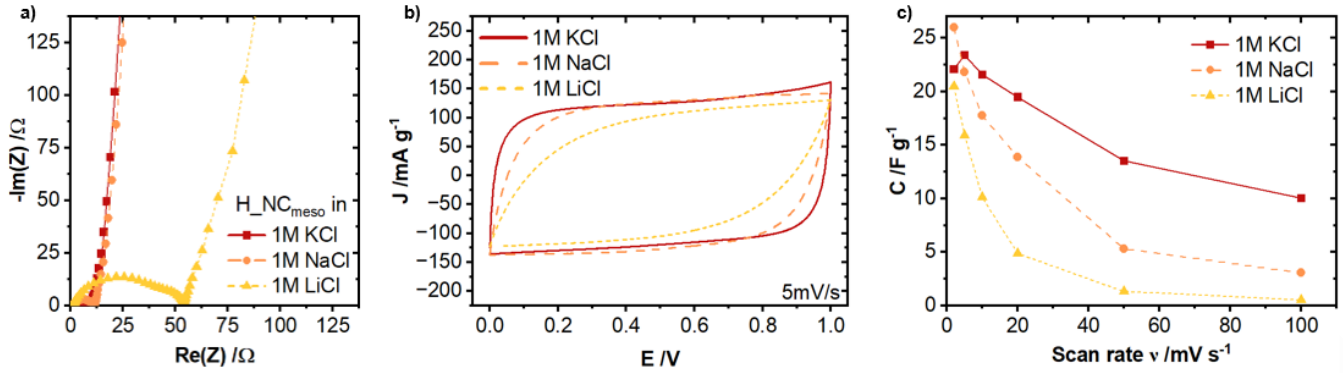

Figure 6: a) PEIS in different aqueous electrolytes. b) CV at scan rate v 5 mV s^{-1} and c) capacitance retention at different scan rates of H_NC_{meso}.

A possible explanation might be the presence of K ions inside the PHI structure in the hybrid, leading to increased double-layer formation due to increased and preferred interaction at the interface. Moreover, the dielectric relaxation constant (Figure S7) support this scan rate behavior. Apparently, the presence of K within the electrode material enhances the final power density of the device.

Comparing the electrochemical of H_NC_{meso} and H_NC_{micro} to other carbon nitride@carbon hybrid materials a capacitance of 23 F g^{-1} at low scan rates is not as potent as other reported materials. Parkin et al. reported a graphitic carbon nitride hybrid with graphene which achieved a specific capacitance up to 266 F g^{-1}.[12] Combining carbon nitrides with other materials such as metal oxides can lead to even better performance.[18] However, the design of a PHI containing hybrid expands the field of carbon nitrides in supercapacitors further and opens further possibilities due to additional metal cations inside the PHI structure and its ionic properties. While it is certainly necessary to improve the electrochemical performance the design of H_NC_{micro} and H_NC_{meso} enables the investigation of K-PHI as active material in EDLCs and potentially other electrochemical storage devices. In the future, the synthesis approach needs to be further optimized in terms of choice of carbon support and K-PHI to carbon ratio among others. Further the PHI itself can also be modified, e.g. with different cations, to alter interaction and impact the performance. Moreover, the investigation of the ionic interactions at the electrified interface will pave the way for the understanding of electric double-layer capacitance in PHIs.

Conclusion

In conclusion, two different hybrid materials were synthesized, incorporating K-PHI into nitrogen-doped porous carbons differing in pore size. Both hybrids have similar chemical properties, however, the larger mesopores in H_NC_{meso} are beneficial to obtain hybrid materials with increased surface area and porosity compared to bulk K-PHI. Both XPS and TEM indicated the growth of K-PHI within the pore structure of H_NC_{meso} whereas for H_NC_{micro} it is most likely present on the external surface area. Electrochemical investigations in a symmetrical supercapacitor setup demonstrated the decreased electric resistance of both hybrid materials resulting in enhanced specific and volumetric capacitance in both hybrids compared to the bulk K-PHI counterpart. Furthermore, it was shown that the formation of K-PHI is beneficial for shorter dielectric relaxation times, which lead to higher capacitance retention for H_NC_{meso} at higher scan rates. Compared to the pristine porous carbons the hybrids show higher power densities. Thus, the hybrid material combines both benefits from the respective bulk materials: higher capacitance than bulk K-PHI due to higher surface area, and higher capacitance at higher scan rates than porous carbons due to the filling of porosity with a semiconducting PHI.

Testing H_NC_{meso} in electrolytes containing other alkali cations than K, namely Na and Li, demonstrated that it is beneficial for the EDLC to match the cations in electrolyte with the cations within the PHI materials. This may originate from an improved interface due to the presence of the same cation species inside the PHI structure. Finally, these hybrid materials will enable the future electrochemical investigation of PHIs and pave the way for their application in other electrochemical applications.

Supporting Information

The authors have cited additional references within the Supporting Information.[26]

Acknowledgements

M. H. and D. L. acknowledge the Fonds der Chemischen Industrie for financial support through the Liebig fellowship. D. L. thanks the Carl-Zeiss-Stiftung for financial support of the project ReAlBatt (P2022-04-046) within the Nexus program. We acknowledge discussions and mentoring from Prof. Dr. Martin Oschatz (Friedrich Schiller University Jena, Institute for Technical Chemistry and Environmental Chemistry. Data and results were partially obtained with the laboratory infrastructure in the working group of Prof. Oschatz. We specifically acknowledge financial support by the European Fonds for Regional Development (Europäischer Fonds für Regionale Entwicklung; EFRE-OP 2021–2027; Project No. 2022 FGI 0007, DyNanoXRD). C.N and A.T. thank TMWWDG FGR 0001 “DeKarbon” for funding. We acknowledge Stephanie Höppener and Ulrich S. Schubert for providing access to the scanning electron microscope. The SEM facilities of the Jena Center for Soft Matter (JCSM) were established with a grant from the DFG.

Keywords: Supercapacitor, Hybrids, Porous Carbon, Carbon nitride, Poly (heptazine imide)

References

[1] M. Castells. *The Information Age: Economy, Society and Culture*; Blackwell, 1996.
[2] A. Savateev, M. Antonietti, *ChemCatChem,* **2019**, *11* (24), 6166-6176.
[3] C. Adler, S. Selim, I. Krivtsov, C. Li, D. Mitoraj, B. Dietzek, J. R. Durrant, R. Beranek, *Adv. Funct. Mater.,* **2021**, *31* (45), 2105369.
[4] H. Schlomberg, J. Kröger, G. Savasci, M. W. Terban, S. Bette, I. Moudrakovski, V. Duppel, F. Podjaski, R. Siegel, J. Senker, R. E. Dinnebier, C. Ochsenfeld, B. V. Lotsch, *Chem. Mater.,* **2019**, *31* (18), 7478-7486.
[5] J. Kröger, A. Jiménez-Solano, G. Savasci, P. Rovó, I. Moudrakovski, K. Küster, H. Schlomberg, H. A. Vignolo-González, V. Duppel, L. Grunenberg, C. B. Dayan, M. Sitti, F. Podjaski, C. Ochsenfeld, B. V. Lotsch, *Advanced Energy Materials,* **2021**, *11* (6), 2003016.
[6] J. Zhang, F. Guo, X. Wang, *Adv. Funct. Mater.,* **2013**, *23* (23), 3008-3014.
[7] A. Savateev, S. Pronkin, M. G. Willinger, M. Antonietti, D. Dontsova, *Chemistry – An Asian Journal,* **2017**, *12* (13), 1517-1522.
[8] M.-Y. Ye, S. Li, X. Zhao, N. V. Tarakina, C. Teutloff, W. Y. Chow, R. Bittl, A. Thomas, *Adv. Mater.,* **2020**, *32* (9), 1903942.
[9] A. Gouder, F. Podjaski, A. Jiménez-Solano, J. Kröger, Y. Wang, B. V. Lotsch, *Energy & Environmental Science,* **2023**, *16* (4), 1520-1530,
[10] J. Kröger, F. Podjaski, G. Savasci, I. Moudrakovski, A. Jiménez-Solano, M. W. Terban, S. Bette, V. Duppel, M. Joos, A. Senocrate, R. Dinnebier, C. Ochsenfeld, B. V. Lotsch, *Adv. Mater.,* **2022**, *34* (7), 2107061.
[11] G. Seo, Y. Saito, M. Nakamichi, K. Nakano, K. Tajima, K. Kanai, *Scientific Reports,* **2021**, *11* (1), 17833.
[12] R. Lin, Z. Li, D. I. Abou El Amaiem, B. Zhang, D. J. L. Brett, G. He, I. P. Parkin, *Journal of Materials Chemistry A,* **2017**, *5* (48), 25545-25554,
[13] Z. Guo, M. Hermesdorf, Y. Chen, P. Feng, Y. Lu, M. Oschatz, D. Leistenschneider, *Electrochim. Acta,* **2025**, *518*, 145751.
[14] Y. Gao, Y. Li, L. Shangguan, Z. Mou, H. Zhang, D. Ge, J. Sun, F. Xia, W. Lei, *J. Colloid Interface Sci.,* **2023**, *644*, 116-123.
[15] J. LIEBIG, *Annalen der Pharmacie,* **1834**, *10* (1), 1-47.
[16] Y. Luo, Y. Yan, S. Zheng, H. Xue, H. Pang, *Journal of Materials Chemistry A,* **2019**, *7* (3), 901-924,
[17] M. Ghaemmaghami, R. Mohammadi, *Sustainable Energy & Fuels,* **2019**, *3* (9), 2176-2204,
[18] P. Chaluvachar, Y. N. Sudhakar, G. T. Mahesha, V. G. Nair, N. Desai, D. K. Pai, *Journal of Energy Chemistry,* **2025**, *103*, 498-524.
[19] W. Niu, Y. Yang, *ACS Energy Letters,* **2018**, *3* (11), 2796-2815.
[20] B. Li, H. Xiong, Y. Xiao, *International Journal of Electrochemical Science,* **2020**, *15* (2), 1363-1377.
[21] E. Frackowiak, *Physical Chemistry Chemical Physics,* **2007**, *9* (15), 1774-1785,
[22] S. Pilathottathil, J. Kavil, M. Shahin Thayyil, *Materials Science and Engineering: B,* **2022**, *276*, 115573.
[23] T. Y. Ma, S. Dai, M. Jaroniec, S. Z. Qiao, *Angew. Chem. Int. Ed.,* **2014**, *53* (28), 7281-7285.
[24] Q. Li, D. Xu, J. Guo, X. Ou, F. Yan, *Carbon,* **2017**, *124*, 599-610.
[25] R. Yan, K. Leus, J. P. Hofmann, M. Antonietti, M. Oschatz, *Nano Energy,* **2020**, *67*, 104240.
[26] C. Schneidermann, C. Kensy, P. Otto, S. Oswald, L. Giebeler, D. Leistenschneider, S. Grätz, S. Dörfler, S. Kaskel, L. Borchardt, *ChemSusChem,* **2019**, *12* (1), 310-319.
[27] M. Thommes, K. Kaneko, A. V. Neimark, J. P. Olivier, F. Rodriguez-Reinoso, J. Rouquerol, K. S. W. Sing, *Pure Appl. Chem.,* **2015**, *87* (9-10), 1051-1069.
[28] I. Krivtsov, D. Mitoraj, C. Adler, M. Ilkaeva, M. Sardo, L. Mafra, C. Neumann, A. Turchanin, C. Li, B. Dietzek, R. Leiter, J. Biskupek, U. Kaiser, C. Im, B. Kirchhoff, T. Jacob, R. Beranek, *Angew. Chem. Int. Ed.,* **2020**, *59* (1), 487-495.
[29] E. Alwin, W. Nowicki, R. Wojcieszak, M. Zieliński, M. Pietrowski, *Dalton Transactions,* **2020**, *49* (36), 12805-12813,
[30] J. Heske, T. D. Kühne, M. Antonietti, *ACS Omega,* **2023**, *8* (29), 26526-26532.
[31] J. K. Brennan, T. J. Bandosz, K. T. Thomson, K. E. Gubbins, *Colloids and Surfaces A: Physicochemical and Engineering Aspects,* **2001**, *187-188*, 539-568.
[32] C. M. Pelicano, J. Li, M. Cabrero-Antonino, I. F. Silva, L. Peng, N. V. Tarakina, S. Navalón, H. García, M. Antonietti, *Journal of Materials Chemistry A,* **2024**, *12* (1), 475-482,
[33] P. L. Taberna, P. Simon, J. F. Fauvarque, *J. Electrochem. Soc.,* **2003**, *150* (3), A292.
[34] B.-A. Mei, O. Munteshari, J. Lau, B. Dunn, L. Pilon, *The Journal of Physical Chemistry C,* **2018**, *122* (1), 194-206.

10.1002/batt.202500285

WILEY VCH

RESEARCH ARTICLE

Entry for the Table of Contents

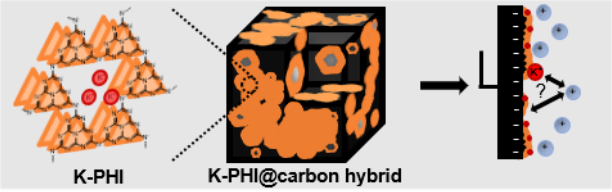

This work highlights the synthesis of a potassium poly(heptazine imide) K-PHI@carbon hybrid material. The design of the hybrid improves the electrochemical properties of the semiconducting carbon nitride enabling the investigation of interaction between K-PHI and different cations from the electrolyte.